

A Novel Thermal Driving Force for Nanodevices

Zeng-Yuan Guo

Quan-Wen Hou

Bing-Yang Cao¹

e-mail: caoby@tsinghua.edu.cn

Key Laboratory for Thermal Science and Power Engineering of Ministry of Education, Department of Engineering Mechanics, Tsinghua University, Beijing 100084, China

Design and construction of nanomotors are one of the most attractive fields in nanotechnology. Following the introduction of a novel concept of the thermomass, the relative mass of a phonon gas based on the Einstein's energy–mass relation, the continuum and momentum conservation equations for the phonon gas are established to characterize the hydrodynamics of the phonon current in a solid. Like the gas flows in the porous mediums, the phonon current in a dielectric solid imposes a driving force on the solid framework atoms, which can be calculated quantitatively and can be applied to actuate nanomotors. We also predict the dynamic behavior of a nanomotor made up of multi-walled carbon nanotubes in terms of molecular dynamics simulations. A shorter single-walled carbon nanotube with a larger diameter, as a mobile part, surrounds a longer single-walled carbon nanotube with a smaller diameter working as a shaft. When a phonon current passes through the inner shaft, the outer nanotube will translate along and/or rotate around the shaft depending on the chiralities of the carbon nanotubes. The motion traces are found to depend on the chirality pair regularly. This type of nanomotor may be promising, because they are directly driven by thermal energy transport.

[DOI: 10.1115/1.4005640]

Keywords: thermal driving force, thermomass theory, carbon nanotube, nanodevice

1 Introduction

Modern nanotechnologies have enabled the fabrication of many nano-electro-mechanical systems (NEMS) with unique attributes, such as small mass, little energy dissipation, and high sensitivity [1–4]. Design and construction of novel NEMS are one of the most attractive objectives in this field. During the past decades, researchers have created a variety of nanodevices, such as nanogenerators driven by biomechanical [5] or acoustic [6] energies, molecular motors by laser [7], light [8] or thermal energy [9], optical and current nanoswitches by electrostatic [10], pH [11] or magnetic [12] fields, and Brownian nanomotors by chemical and biogenic energies [13–15]. The operation of all these nanodevices is at the expense of certain power input and actuation. Seeking new actuation mechanisms is one of the central missions for the next generation nanodevices.

More recently, a temperature gradient was found to be able to cause a driving force. Barreiro et al. [16] are the first to observe experimentally that imposing a temperature gradient along an inner carbon nanotube could drive an outer nanotube to rotate and/or translate. They then indicated that the thermal gradient generated a phonon current in the inner tube that hit and dragged the outer tube. Motions of gold nanoparticles and water nanodroplets confined inside carbon nanotubes (CNTs) subject to temperature gradients were also observed by molecular dynamics (MD) simulations. It physical mechanism was then attributed to thermophoresis [17–19]. In the MD simulations of Shiomi et al., however, the mass transport of a water cluster inside a carbon nanotube with a temperature gradient was demonstrated to be caused by the temperature dependence of the potential energy of the confined water [20]. We can see that the phonon current can result in a driving force and serve as a promising actuation for nanomotors. Further studies on its physical mechanism and mathematical characterization are highly desired.

The phonon current induced actuation should relate to the hydrodynamics of the phonon gas motion in a dielectric, which

was recently established by Guo and Cao [21,22]. The mass of a phonon gas, called thermomass, was defined as the equivalent mass of its energy based on Einstein's mass–energy relation. Heat conduction in solids was due to the motion of the thermomass. These concepts were used to establish the mass and momentum conservation equations for the thermomass including the driving, inertial, and resistant forces using Newtonian mechanics. The conservation equations are just a general law of heat conduction derived from the first principle. The general law degenerates to Fourier's law of heat conduction when the inertial force could be neglected relative to the other terms so that the heat conduction became pure diffusion. However, Fourier's law of heat conduction no longer held if the heat flux was very high, such that the inertial force of the phonon gas was not negligible. This thermomass concept based theory presents us a hydrodynamic image of the phonon current in a solid.

Here, we further focus on the motion of the phonon gas motion in a solid on the basis of the thermomass theory. The physical mechanism of the temperature gradient induced driving force of nanomotors is found to be just the drag caused by the weighty phonon current, which can be characterized by the conservation equations for the phonon gas motion quantitatively. Thermally driven nanomotors made up of multiwalled carbon nanotubes are then designed in terms of molecular dynamics simulations. A shorter single-walled carbon nanotube with a larger diameter, as a mobile part, surrounds a longer single-walled carbon nanotube with a smaller diameter working as a shaft. When a phonon current passes through the inner shaft, the outer nanotube will translate along and/or rotate around the shaft depending on the chiralities of the carbon nanotubes.

2 Theoretical Analysis

2.1 Equivalent Mass of Phonon Gas. The thermal energy in a solid is due to the thermal vibration energy in lattices. The lattice vibration energy can be quantized and the energy quantum is called phonon. The state of the lattice vibrations may be characterized by the phonon gas consisting of large numbers of phonons moving randomly [23]. According to Einstein's mass–energy relation [24], the mass of an object increases with its speed. The relation can be used in the thermal motion of molecules or/and lattices [25,26]. As

¹Corresponding author.

Contributed by the Heat Transfer Division of ASME for publication in the JOURNAL OF HEAT TRANSFER. Manuscript received April 19, 2010; final manuscript received May 10, 2010; published online April 11, 2012. Assoc. Editor: Ping Cheng.

the velocities of the lattice vibrations are much less than the speed of light, the equivalent mass of a phonon gas, called thermomass, can be defined as [21]

$$M_h = \frac{E_{D0}}{c^2} \quad (1)$$

in which M_h is the thermomass, E_{D0} is the energy of the phonon gas, and c is the speed of light in vacuum. The thermomass in a unit volume is then referred to as a thermomass density

$$\rho_h = \frac{\rho CT}{c^2} \quad (2)$$

in which ρ_h is the thermomass density, ρ is the density of rest mass, C is the specific heat, and T is the temperature.

Since the phonon gas has the nature of mass according to Einstein's mass-energy relation, and the heat transport is actually the motion of the phonon gas, the phonon gas may be regarded as a kind of weighty fluid unlike the caloric theory. The thermal motion of the phonons results in a pressure on the interfaces of an object. This pressure supplements the traditional pressure arising from the rest mass of lattices. The state equation of a phonon gas was deduced from the Debye state equation by Guo et al. [27]. The Debye state equation for solids is

$$p = -\frac{\partial E}{\partial V} + \frac{\gamma E_{D0}}{V} \quad (3)$$

in which p is the pressure, V is the volume, E_{D0} is the lattice vibration energy, i.e., thermal energy of the solid, and γ is the Grüneisen constant. The first term on the right-hand side of Eq. (3) which represents the interactions between atoms is negative attractive force. The second term due to the lattice vibrations is a positive repulsive force. Since this force arises from thermal vibrations, it can be called thermal mass pressure or phonon gas pressure. The phonon gas pressure can then be related to the energy by the state equation of a phonon gas as

$$p_h = \gamma \rho_h CT = \frac{\gamma \rho}{c^2} (CT)^2 \quad (4)$$

The phonon gas pressure is proportional to the square of the temperature, since the phonon gas mass is proportional to the temperature. Just as the pressure gradient is the driving force for the fluid flow, the driving force for the phonon gas motion in solids is the pressure gradient of the phonon gas.

2.2 Hydrodynamics of Thermomass Motion. One of macroscopic modelizations of phonon heat conduction is called phonon hydrodynamics [28–30]. It shows that the transport of phonons in a solid is really like fluid flows in channels. The previous phonon hydrodynamics is based on solving linearized Boltzmann equations of phonons. Here, based on introducing the concept of thermomass for the phonon gas, we can establish the conservation equations to characterize the hydrodynamics of phonon gas in a solid using Newtonian mechanics.

When a temperature gradient occurs in a solid, thermal energy flows from the hot to the cold regions. The rate of the thermal energy transport is usually described by the heat flux through Fourier's law

$$q = -K \frac{dT}{dx} \quad (5)$$

in which T is the temperature and q is the heat flux. The thermal energy motion can be better described by its velocity defined as

$$q = \rho CT u_h \quad (6)$$

where u_h is the drift velocity. Since the thermal energy in a solid is equal to the energy of the phonon gas, ρCT is actually the

energy of the phonon gas per unit volume. Thus, u_h is the velocity of the thermal energy motion, which is equivalent to the mean phonon drift velocity or the macroscopic directional velocity of the phonon gas.

Just as the pressure gradient is the driving force for the fluid flow, the driving force for the phonon gas motion in solids is the pressure gradient of the phonon gas. For a one dimensional case, the pressure gradient on the phonon gas can be written as

$$\frac{dp_h}{dx} = \frac{\gamma \rho C^2}{c^2} \frac{d(T^2)}{dx} = \frac{2\gamma \rho C^2}{c^2} T \frac{dT}{dx} \quad (7)$$

Therefore, the driving force for the phonon gas motion is proportional to the gradient of the square of the temperature. The temperature gradient is often understood as the driving force for the heat flux. Since the temperature gradient does not have a unit of force, it is called a generalized force or thermodynamic force in irreversible thermodynamics, with the heat flux treated as a generalized flux driven by the generalized force. Unlike this conventional viewpoint, the driving force for the heat conduction here is a real force in the unit of N.

When the phonon gas drifts in a solid, the driving force should be counterbalanced by a resistant force. The drift of phonons is similar to fluid flow in porous media, where the resistant force is proportional to the fluid velocity. For phonons drifting in a solid, the resistance induced by the phonon scattering can also be related to the drift velocity by a linear relation

$$f_h = \beta_h u_h \quad (8)$$

with a proportionality coefficient [21]

$$\beta_h = \frac{2\gamma c^2 C \rho_h^2}{K} \quad (9)$$

For heat transport in a solid without an internal heat source, the equivalent mass of the phonon gas remains constant during the motion of the phonon gas. The continuity equation is

$$\frac{\partial \rho_h}{\partial t} + \text{div}(\rho_h U_h) = 0 \quad (10)$$

The continuity equation for one dimensional, steady state thermal conduction can be simplified to

$$\rho_h u_h = \text{const} \quad (11)$$

Because the density of the phonon gas in a solid varies along with temperature, the phonon gas accelerates along the flow direction. This results in an inertial force of the phonon gas due to the velocity variation in the direction of heat flow even for steady state cases.

As stated above, the driving force for heat transport is the pressure gradient in the phonon gas. The momentum variation in the phonon gas results in an inertial force. The momentum here refers to the momentum carried by the equivalent mass of the phonon gas, which differs from the apparent momentum of a phonon defined in solid physics. In addition, a resistance must exist because of the nonlinearity of the lattice vibrations and defects in the solid. Thus, the momentum conservation equation of motion for the phonon gas can be written as in fluid mechanics

$$\rho_h \frac{DU_h}{Dt} + \nabla p_h + f_h = 0 \quad (12)$$

Here, the first term represents the inertial force of the phonon gas motion, the second term is the pressure gradient, and the third term is the resistance.

For one dimensional heat conduction cases, combining Eqs. (10) and (12) gives the following heat conduction law:

$$\tau_m \left[\frac{\partial q}{\partial t} + u_h \frac{\partial(\rho CT)}{\partial t} \right] + \tau_m u_h \left[\frac{\partial q}{\partial x} - u_h \frac{\partial(\rho CT)}{\partial x} \right] + K \frac{\partial T}{\partial x} + q = 0 \quad (13)$$

in which

$$\tau_m = \frac{K}{2\gamma\rho C^2 T} \quad (14)$$

Here, all the first four terms in the left-hand side of Eq. (13) represent the inertial force of the phonon gas motion, the fifth term is the pressure gradient, and the sixth term is the resistance. τ_m is a characteristic time and represents the damping attribute of an object. With ignoring the four inertial terms, Eq. (13) will reduce to Fourier's law of heat conduction. Therefore, the physical essence of Fourier's law of heat conduction is the motion of a phonon gas when its driving force (or pressure gradient) is in balance with its resistant force. In other words, Fourier's law characterizes the thermal energy motion as the pressure gradient is counterbalanced by the resistance. With ignoring the second to fourth terms, Eq. (13) will then degenerate to Cattaneo-Vernotte (CV) model, a thermal wave model named by Cattaneo [31] and Vernotte [32]. Since Eq. (13) is on the basis of the first principle and without traditional hypotheses in heat conduction processes, it is just a general heat conduction law with wider applicability than Fourier's heat conduction law and CV model.

2.3 Actuation by Phonon Current. When the thermomass fluid flows in a solid subject to a temperature gradient, there are three kinds of force acting on the thermomass: the driving, inertial, and resistant forces. From the principle of mechanics, the resultant force of the three forces must be zero. The ratio of the inertial force to the driving force can be written as

$$\xi = \frac{q^2}{2\gamma\rho^2 C^3 T^3} \quad (15)$$

The ratio is very small under normal heat conduction conditions. For one dimensional heat conduction through a silicon plate with boundary temperatures $T_1 = 400$ K and $T_2 = 300$ K and a heat flux of $q = 10^4$ W/m², the velocity of the phonon gas is only about 10^{-5} m/s and the ratio of the inertial force to the driving force is only on the order of 10^{-16} . In this case, the resistant force is equal to the driving force. The transport of the phonon gas is blocked by such a resistant force as a balance force of the driving force. Meanwhile, the thermomass fluid must act an equal counteracting force on the framework atoms. If the solid atoms are moveable, the solid will displace. This is just the physical mechanism of the actuation induced by the phonon current. Equal to the gradient of the phonon gas pressure, the phonon current induced driving force, which acts on the framework atoms in a unit volume, is

$$f_{dv} = \frac{2\gamma\rho C^2}{c^2} T \frac{dT}{dx} \quad (16)$$

This image is similar to the electromigration in which vacancies, driven by an electron wind, may move [33,34].

We now turn our attention to the phonon current induced actuation from both the macroscopic and microscopic viewpoints. From the macroscopic point of view, the standard treatment of irreversible thermodynamics shows that a thermal gradient must give a mass flow [35]. The thermal gradient driven diffusion between two fluids is called Soret effect [36]. The solid particle displacement in a fluid driven by a thermal gradient is often called

thermophoresis [37]. The point is made here that the heat flow induced driving force contributes to the thermal gradient induced mass flow, partially at least. From the microscopic point of view, on the other hand, the phonon scattering by lattices can give rise to mass transport in a matter. Though the phonons are often regarded as only carrying pseudomomentum in solid state physics, there are a number of interactions of phonons with particles possessing real momenta, such as electrons, photons [38]. The conservation of real momentum was said to be accomplished through changes in the momentum of zero wave number. Moreover, the existence of an elastic radiation pressure equal to one third of the elastic energy density implies for all practical considerations every phonon of energy $h\nu$ has associated with it an effective real momentum of magnitude h/λ , in which h is the Planck constant, ν is the frequency, and λ is the wave length [39]. The momentum transfer between phonons and lattices just gives rise to the phonon current induced driving force.

Why can we not observe that an ordinary object move under the action of a phonon current? One reason is that the conductor often is restricted by the substrates. Another is that the driving force is often too small to drive an object to move. In nanotechnologies, however, the phonon current induced force is expected to play an important role in nanomotors owing to the superhigh heat flux and ultrasmall object mass.

Carbon nanotubes are one of the best components for designing such thermally driven nanomotors. First, the thermal conductivity of carbon nanotubes is very large (larger than 3000 W/mK [40–43]) so that a small temperature difference may give rise to a large heat flux. Second, the friction between layers in multiwalled carbon nanotubes has been found to be very small due to the weak interaction between interlayer atoms in the form of Van der Waals [44,45]. Barreiro et al. [16] in their experiments found that a temperature gradient could give rise to a subnanometer displacement of a carbon nanotube cargo. When there was a phonon current, an outer nanotube might translate along or rotate around the inner tube.

We now calculate the phonon current induced driving force in CNTs based nanomotors like in Ref. [16]. The outer and inner nanotubes are assumed to have the same temperature gradient since their relative velocity is very small in micrometer per second order of magnitude. Driven by the phonon current, the outer nanotube will move to the downstream of the heat flow. Based on Eq. (16), the resistant force is equal to the driving force when the motion reaches a steady state. For a given volume, V , of framework atoms, we have

$$f_{dm} = V f_{dv} = \frac{2\gamma m C^2 T q}{K c^2} \quad (17)$$

in which m is the mass of the outer carbon nanotube. In the experiments of Barreiro et al. [16], the mean temperature gradient is about 1 K/nm, the mass of the outer nanotube can be figured out $m \approx 10^{-17}$ kg. Taking the system temperature as $T = 300$ K, the Grüneisen constant $\gamma = 1$, and the heat capacity as $C = 500$ J/kg K, the driving force induced by the phonon current is $F \approx 10^{-17}$ N.

Servantie and Gaspard [46] put forward a theory to predict the friction between carbon nanotube layers related to their relative velocity

$$f_r = N\Gamma v \quad (18)$$

in which f_r is the friction, N is the atom number covered by a contact area, v is the relative velocity, Γ is a proportionality constant that is about 10^{-16} m/s/atom for carbon nanotubes. We can estimate the contacting atom number is about $N \sim 10^4$ in the experiments of Barreiro et al. Then, the friction is estimated to be in the order of $f_r \approx 10^{-18}$ N of magnitude. It is in a good agreement with the prediction by our thermomass concept based theory above.

3 CNTs Based Nanomotors

3.1 MD Simulation Details. The simulated nanomotor is consisted of a short outer tube and a long inner tube, i.e., a double-walled carbon nanotube (DWNT), as shown in Fig. 1. The two ends of the inner tube are fixed. The regions adjacent to the fixed ends are attached to Nose–Hoover thermostats to be maintained at different temperatures, respectively. Actuated by this temperature difference, the outer tube moves along and around the inner tube, in other words, the thermally driven nanomotor operates. In this CNTs based nanomotor, the outer tube acts as a movable component and the inner tube serves as a shaft. Such a nanomotor has been demonstrated to be able to work by recent experiments [16], which yield a firm engineering background for our MD simulations. Furthermore, the potential patterns play a dominant role in the motion behaviors of the nanomotor, since the driving force induced by the temperature gradient is very small. The Verlet leap-frog scheme is applied to integrate the motion equations with a time step of 2 fs [47]. The thermal transport in the simulation system is established during a run of 200 ps, while the outer tube is restricted from moving rotationally and translationally by rescaling the velocities of its atoms. After the restriction is removed, the outer tube moves under the action of the inner tube.

In our MD simulations, the intrawall C-C bonds are modeled by the bond-order potential developed by Brenner [48]

$$E = \sum_i \sum_{j(>i)} [V_R(r_{ij}) - b_{ij}V_A(r_{ij})] \quad (19)$$

where $V_R(r)$ and $V_A(r)$ denote the pair-additive repulsive and attractive interactions, respectively, and b_{ij} represents a many-body coupling between the bond from atom i to atom j and the local environment. The interwall interactions between the carbon atoms are via the Lenard–Jones potential in the form of

$$V(r) = 4\epsilon \left[\left(\frac{\sigma}{r} \right)^{12} - \left(\frac{\sigma}{r} \right)^6 \right] \quad (20)$$

in which $\epsilon = 2.968$ meV, $\sigma = 0.3407$ nm [49].

3.2 Operation Behaviors. Three DWNTs based nanomotors with different chirality pairs are simulated as tabulated in Table 1. The interwall distance in all the systems is about 0.34 nm which ensures the stability of the structure and movement. The potential patterns of the three DWNT systems are plotted in Fig. 2. The two degrees of freedom of motion are taken to be sliding along the nanotube axis and rotation around the nanotube axis. A darker color denotes a lower potential energy. Allowing for the difference in DWNTs' lengths, the potential patterns calculated in this paper are quantitatively in agreement with the results in Refs. [49]

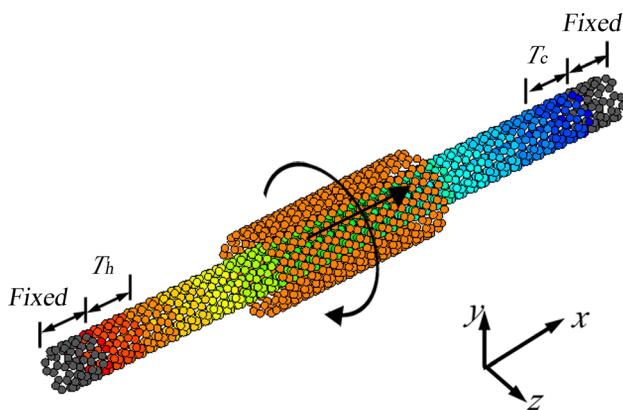


Fig. 1 Schematic of the nanomotor constructed by a DWNT

Table 1 Structural parameters of three DWNTs based nanomotors

Case	Chirality pair	Length (nm)	Radius (nm)	Interwall distance (nm)
1	(5, 5)/(10, 10)	24.9/7.5	0.344/0.688	0.344
2	(13, 0)/(22, 0)	25.9/5.2	0.516/0.873	0.357
3	(8, 2)/(17, 2)	26.4/5.2	0.364/0.718	0.354

and [50]. If the outer tube is completely released, it will fall into the potential valleys with the lowest energy. Driven by a small force, it will choose an easy way, which is just the minimum energy track, to move. The minimum energy tracks of the (5, 5)/(10, 10), (13, 0)/(22, 0), and (8, 2)/(17, 2) nanomotors are along the tube axis, circumference and helix, respectively, as illustrated in Fig. 2. Between two neighbor minimum energy tracks are a potential barriers ΔU , which are the restriction ability from changing tracks for the outer tube. The barriers of case 1, 2, and 3 in our simulations are 0.024 eV, 0.15 eV, and 0.12 eV, respectively.

With the two ends of the inner tube being at 600 K and 400 K, the outer tube will speed up, namely, the thermally driven nanomotor will run. The center of the mass and the rotation angle along the circumference of the outer tube varying with time are shown in Fig. 3. Driven by the temperature difference, the outer tubes of all the three nanomotors move toward the specific directions. This phenomenon is similar to that observed in the experiments and simulations by Barreiro et al. [16]. Its actuation mechanism can be understood by considering the drag on the outer tube induced by the phonon current transporting in the nanomotor as stated above. For the (5, 5)/(10, 10) nanomotor as shown in Fig. 3(a), the outer tube translates along the axis and oscillates in the circumferential direction. The maximum oscillation amplitude is about 15 deg, less than the separation angle between two neighbor minimum energy tracks in the (5, 5)/(10, 10) DWNTs. It indicates that the movement of the outer tube is confined in the minimum energy tracks as shown in Fig. 2(a). The same conclusion can be drawn for the (13, 0)/(22, 0) DWNT (Fig. 3(b)) in which the outer tube rotates around the axis with very small oscillations in the axis direction (less than 0.06 nm). In this case,

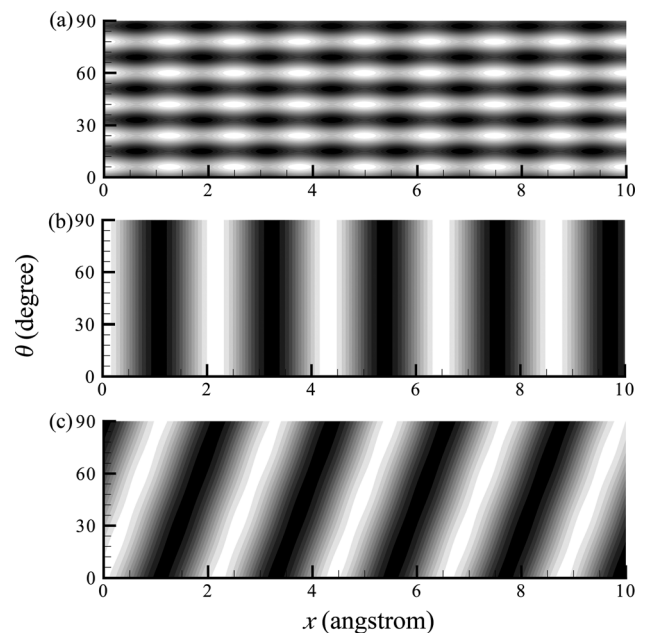


Fig. 2 Interwall potential patterns for DWNTs with different chirality pairs: (a) (5, 5)/(10, 10), (b) (13, 0)/(22, 0), and (c) (8, 2)/(17, 2)

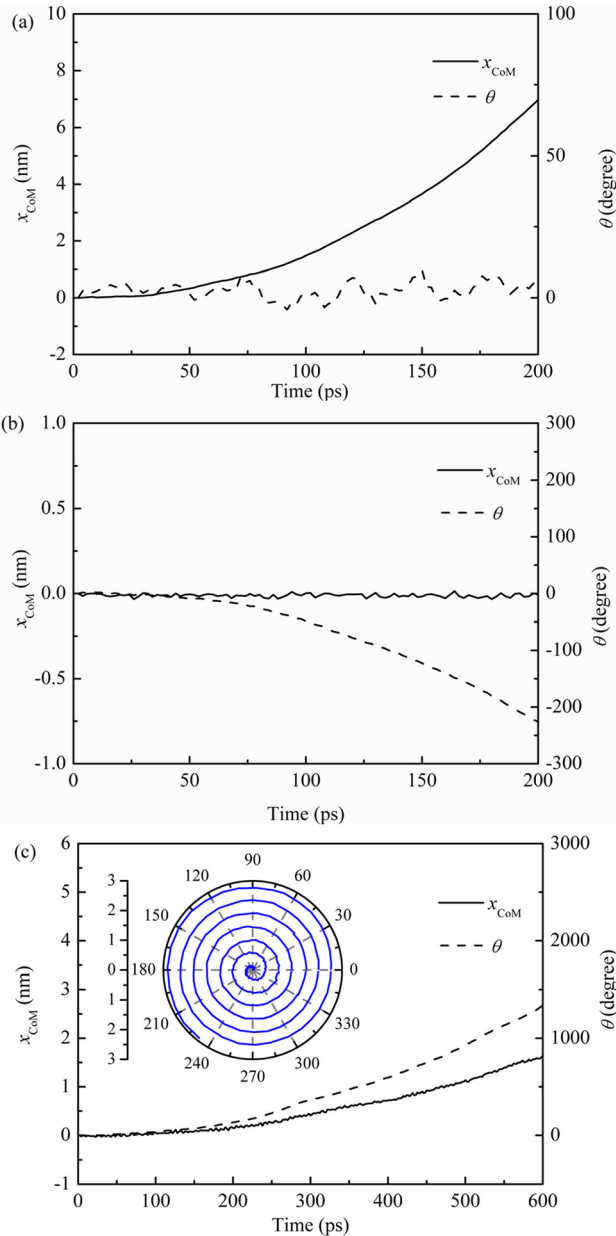


Fig. 3 The center of mass and the rotation angle of the outer tube varying with time for: (a) (5, 5)/(10, 10), (b) (13, 0)/(22, 0), and (c) (8, 2)/(17, 2). The inset in (c) plots the trace of the motion in a polar coordinate system, whose polar axis and angle units are nanometer and degree, respectively.

however, we should point out that because of the perpendicularity between the minimum energy track and the thermal driving force, the rotation direction of the outer tube, that is, clockwise or anti-clockwise, depends on the initial actuation. The minimum energy track in the (8, 2)/(17, 2) DWNT has been demonstrated to be a helix above. For this nanomotor, Fig. 3(c) shows the trace of the outer tube, and the inset gives the rotation angle as a function of the translational distance in a polar coordinate system. The rotational angle is proportional to the translational distance, indicative of a helix trace. The helix angle of the trace is 810 ± 9.8 deg/nm, which agrees with the helix angle of the minimum energy tracks, 829 deg/nm obtained by Fig. 2(c). The small deviation may arise from the deformation of the tubes at different temperatures. Therefore, the motion in this system is also consistent with the minimum energy tracks. Under the current conditions, the thermally driven nanomotors run along the minimum energy tracks with specific directions depending on the DWNT chirality pairs.

From this point of view, the directional control of DWNTs based nanodevices can be realized.

4 Conclusion

Based on introducing a novel concept called thermomass, the relativistic mass of a phonon gas in light of the Einstein's energy-mass relation, the continuum and momentum conservation equations for the phonon gas are established to characterize the hydrodynamics of the phonon current in a solid. There are three types of force acting on the phonon gas simultaneously: driving force, inertial force, and resistance. The counteracting force of the resistance, like the gas flows in the porous mediums, gives rise to a driving force on the solid framework atoms, which can be calculated quantitatively and can be applied to actuate nanomotors. The dynamic behaviors of a nanomotor made up of multiwalled carbon nanotubes are then investigated by using molecular dynamics simulations. A shorter single-walled carbon nanotube with a larger diameter, as a mobile part, surrounds a longer single-walled carbon nanotube with a smaller diameter working as a shaft. When a phonon current passes through the inner shaft, the outer nanotube will translate along or rotate around the shaft depending on the chiralities of the carbon nanotubes. The motion traces are found to depend on the chirality pair regularly and are confined within the minimum energy track of the CNT potential patterns, which implies that the motion direction of the CNTs based nanomotors can be controlled. This makes such a type of nanomotor more promising.

Acknowledgment

This work is financially supported by National Natural Science Foundation of China (Nos. 51136001, 50976052, 50606018), Tsinghua National Laboratory for Information Science and Technology (TNList) Cross-discipline Foundation, and the Tsinghua University Initiative Scientific Research Program.

Nomenclature

- b_{ij} = many-body coupling between C-C bond from atom i to atom j
- c = speed of light in vacuum (m/s)
- C = specific heat (J/kg · K)
- E = potential energy between atoms (J)
- E_{DO} = energy of phonon gas (J)
- f_{dV} = thermal driving force in unit volume (N/m³)
- f_h = resistance (N)
- f_r = friction (N)
- K = thermal conductivity (W/m K)
- m = mass (kg)
- M_h = thermomass (kg)
- N = atom number
- p = pressure (Pa)
- p_h = phonon gas pressure (Pa)
- q = heat flux (W/m²)
- r = distance (m)
- T = temperature (K)
- u_h = drift velocity of phonon gas (m/s)
- v = velocity (m/s)
- V = volume (m³)
- V_A = attractive potential energy (J)
- V_R = repulsive potential energy (J)

Greek Symbols

- β_h = resistance coefficient (kg/s)
- σ = atom diameter (m)
- ε = potential well (J)
- ρ = density of rest mass (kg/m³)
- ρ_h = thermomass density (kg/m³)
- γ = Grüneisen constant
- τ_{tm} = characteristic time (s)
- ξ = ratio of inertial force to driving force
- Γ = proportionality constant (m/s atom)

Subscripts

A = attractive
 d = driving
 D_0 = thermal energy
 h = thermomass
 ij = from atom i to atom j
 r = friction
 R = repulsive
 V = unit volume

References

- [1] Hsu, T. R., 2002, *MEMS and Microsystems: Design and Manufacture*, McGraw-Hill, Boston.
- [2] Craighead, H. G., 2000, "Nanoelectromechanical Systems," *Science*, **290**, pp. 1532–1535.
- [3] Roukes, M., 2001, "Nanoelectromechanical Systems Face the Future," *Phys. World*, **14**, pp. 25–31.
- [4] Ekinci, K. L., and Roukes, M. L., 2005, "Nanoelectromechanical Systems," *Rev. Sci. Instrum.*, **76**, p. 061101.
- [5] Yang, R., Qin, Y., Li, C., Zhu, G., and Wang, Z. L., 2009, "Converting Biomechanical Energy Into Electricity by a Muscle-Movement-Driven Nanogenerator," *Nano Lett.*, **9**, pp. 1201–1205.
- [6] Insepov, Z., Wolf, D., and Hassanein, A., 2006, "Nanopumping Using Carbon Nanotubes," *Nano Lett.*, **6**, pp. 1893–1895.
- [7] Tuzun, R. E., Noid, D. W., and Sumpter, B. G., 1995, "Dynamics of a Laser Driven Molecular Motor," *Nanotechnology*, **6**, pp. 52–63.
- [8] Torras, J., Rodriguez-Ropero, F., Bertran, O., and Aleman, C. J., 2009, "Controlled Isomerization of a Light-Driven Molecular Motor: A Theoretical Study," *J. Phys. Chem. C*, **113**, pp. 3574–3580.
- [9] Somada, H., Hirahara, K., Akita, S., and Nakayama, Y., 2009, "A Molecular Linear Motor Consisting of Carbon Nanotubes," *Nano Lett.*, **9**, pp. 62–65.
- [10] Alu, A., and Egheta, N., 2009, "Optical Nanoswitch: An Engineered Plasmonic Nanoparticle With Extreme Parameters and Giant Anisotropy," *New J. Phys.*, **11**, p. 013026.
- [11] Liu, D. S., Bruckbauer, A., Abell, C., Balasubramanian, S., Kang, D. J., Klenerman, D., and Zhou, D. J., 2006, "A Reversible pH-Driven DNA Nanoswitch Array," *J. Am. Chem. Soc.*, **128**, pp. 2067–2071.
- [12] Cresti, A., 2008, "Proposal for a Graphene-Based Current Nanoswitch," *Nanotechnology*, **19**, p. 265401.
- [13] Astumian, D., and Hanggi, P., 2002, "Brownian Motors," *Phys. Today*, **11**, pp. 33–39.
- [14] Hanggi, P., and Marchesoni, F., 2009, "Artificial Brownian Motors: Controlling Transport on the Nanoscale," *Rev. Mod. Phys.*, **81**, pp. 387–442.
- [15] Omabegho, T., Sha, R., and Seeman, N. C., 2009, "A Bipedal DNA Brownian Motor With Coordinated Legs," *Science*, **324**, pp. 67–71.
- [16] Barreiro, A., Ruruli, R., Hernández, E. R., Moser, J., Pichler, T., Forró, L., and Bachtold, A., 2008, "Subnanometer Motion of Cargoes Driven by Thermal Gradients Along Carbon Nanotubes," *Science*, **320**, pp. 775–778.
- [17] Schoen, P. A. E., Walther, J. H., Arcidiacono, S., Poulikakos, D., and Koumoutsakos, P., 2006, "Thermophoretic Motion of Water Nanodroplets Confined Inside Carbon Nanotubes," *Nano Lett.*, **9**, pp. 1910–1917.
- [18] Schoen, P. A. E., Walther, J. H., Poulikakos, D., and Koumoutsakos, P., 2007, "Phonon Assisted Thermophoretic Motion of Gold Nanoparticles in Carbon Nanotubes," *Appl. Phys. Lett.*, **90**, p. 253116.
- [19] Zambrano, H. A., Walther, J. H., Koumoutsakos, P., and Sbalzarini, I. F., 2009, "Thermophoretic Motion of Water Nanodroplets Confined Inside Carbon Nanotubes," *Nano Lett.*, **9**, pp. 66–71.
- [20] Shiomi, J., and Maruyama, S., 2009, "Water Transport Inside a Single-Walled Carbon Nanotube Driven by a Temperature Gradient," *Nanotechnology*, **20**, p. 055708.
- [21] Cao, B. Y., and Guo, Z. Y., 2007, "Equation of Motion of Phonon Gas and Non-Fourier Heat Conduction," *J. Appl. Phys.*, **102**, p. 053503.
- [22] Guo, Z. Y., and Cao, B. Y., 2008, "A General Heat Conduction Law Based on the Concept of Motion of Thermal Mass," *Acta Phys. Sin.*, **57**, pp. 4273–4281.
- [23] Kittel, C., Xiang, J. Z., and Wu, X. H., 2005, *Introduction to Solid State Physics*, Chemical Industry Press, Beijing.
- [24] Einstein, A., Lorentz, H. A., Minkowski, V., and Weyl, H., 1952, *The Principle of Relativity*, Dover publications, New York.
- [25] Feynman, R. P., Leighton, R. B., and Sands, M. L., 1963, *The Feynman Lectures on Physics*, Addison-Wesley, Boston.
- [26] Young, H. D., and Freedman, R. A., 2004, *Sears and Zemansky's University Physics: With Modern Physics*, 11th ed., Pearson Addison Wesley, San Francisco.
- [27] Guo, Z. Y., Cao, B. Y., Zhu, H. Y., and Zhang, Q. G., 2007, "State Equation of Phonon Gas and Conservation Equations for Phonon Gas Motion," *Acta Phys. Sin.*, **56**, pp. 3306–3312.
- [28] Guyer, R. A., and Krumhansl, J. A., 1966, "Thermal Conductivity, Second Sound, and Phonon Hydrodynamic Phenomena in Nonmetallic Crystals," *Phys. Rev.*, **148**, pp. 778–788.
- [29] Cimmelli, V. A., and Frischmuth, K., 2007, "Gradient Generalization to the Extended Thermodynamic Approach and Diffusive-Hyperbolic Heat Conduction," *Physica B*, **400**, pp. 257–265.
- [30] Alvarez, F. X., Jou, D., and Sellitto, A., 2009, "Size and Frequency Dependence of Effective Thermal Conductivity in Nanosystems," *J. Appl. Phys.*, **105**, p. 014317.
- [31] Cattaneo, C., 1948, "On the Conduction of Caloric," *Atti. Semin. Mat. Fis. Univ. Modena*, **3**, pp. 83–101.
- [32] Vernotte, P. C. R., 1958, "Paradoxes of the Continuous Theory of the Heat Equation," *Acad. Sci.*, **246**, pp. 3154–3155.
- [33] Lloyd, J. R., 1997, "Electromigration in Thin Film Conductors," *Semicond. Sci. Technol.*, **12**, pp. 1177–1185.
- [34] Tu, K. N., 2003, "Recent Advances on Electromigration in Very-Large-Scale-Integration of Interconnects," *J. Appl. Phys.*, **94**, pp. 5451–5473.
- [35] Denbigh, K. G., 1951, *The Thermodynamics of the Steady State*, Methuen, London.
- [36] Soret, C. H., 1879, "Sur L'état D'équilibre Que Prend, du Point de vue de sa Concentration, une Dissolution Saline Primitivement Homogène, dont deux Parties sont Portées à des Températures Différentes," *Arch. De Geneve*, **3**, pp. 48–61.
- [37] Goldhirsch, I., and Ronis, D., 1983, "Theory of Thermophoresis. I. General Considerations and Modecoupling Analysis," *Phys. Rev. A*, **27**, pp. 1616–1634.
- [38] Stokes, H. T., 1987, *Solid State Physics*, Allyn and Bacon, Boston.
- [39] Huntington, H. B., 1968, "Driving Forces for Thermal Mass Transport," *J. Phys. Chem. Solids*, **29**, pp. 1641–1651.
- [40] Berber, S., Kwon, Y. K., and Tomanek, D., 2000, "Unusually High Thermal Conductivity of Carbon Nanotubes," *Phys. Rev. Lett.*, **84**, pp. 4613–4616.
- [41] Hou, Q. W., Cao, B. Y., and Guo, Z. Y., 2009, "Thermal Conductivity of Carbon Nanotube: From Ballistic to Diffusive Transport," *Acta Phys. Sin.*, **58**, pp. 7809–7814.
- [42] Pop, E., Mann, D., Wang, Q., Goodson, K., and Dai, H., 2006, "Thermal Conductance of an Individual Single-Wall Carbon Nanotube Above Room Temperature," *Nano Lett.*, **6**, pp. 96–100.
- [43] Fujii, M., Zhang, X., Xie, H. Q., Ago, H., Takahashi, K., Ikuta, T., Abe, H., and Shimizu, T., 2005, "Measuring the Thermal Conductivity of a Single Carbon Nanotube," *Phys. Rev. Lett.*, **95**, p. 065502.
- [44] Cumings, J., and Zettl, A., 2000, "Low-Friction Nanoscale Linear Bearing Realized From Multiwall Carbon Nanotubes," *Science*, **289**, pp. 602–604.
- [45] Yu, M. F., Yakobson, B. I., and Ruoff, R. S., 2000, "Controlled Sliding and Pullout of Nested Shells in Individual Multiwalled Carbon Nanotubes," *J. Phys. Chem. B*, **104**, pp. 8764–8767.
- [46] Servantie, J., and Gaspard, P., 2003, "Methods of Calculation of a Friction Coefficient: Application to Nanotubes," *Phys. Rev. Lett.*, **91**, p. 185503.
- [47] Allen, M. P., and Tildesley, D. J., 1987, *Computer Simulation of Liquids*, Clarendon, Oxford.
- [48] Brenner, D. W., 1990, "Empirical Potential for Hydrocarbons for Use in Simulating the Chemical Vapor Deposition of Diamond Films," *Phys. Rev. B*, **42**, pp. 9458–9471.
- [49] Saito, R., Matsuo, R., Kimura, T., Dresselhaus, G., and Dresselhaus, M. S., 2001, "Anomalous Potential Barrier of Double-Wall Carbon Nanotube," *Chem. Phys. Lett.*, **348**, pp. 187–193.
- [50] Lozovik, Y. E., Minogin, A., and Popov, A. M., 2003, "Nanomachines Based on Carbon Nanotubes," *Phys. Lett. A*, **313**, pp. 112–121.